9-1-2011

Truncation of the Mrp20 Protein Reveals New Ribosome-assembly Subcomplex in Mitochondria

Jasvinder Kaur
Marquette University

Rosemary A. Stuart
Marquette University, rosemary.stuart@marquette.edu

Truncation of the Mrp20 protein reveals new ribosome-assembly subcomplex in mitochondria

Jasvinder Kaur

Department of Biological Sciences, Marquette University
Milwaukee, WI

Rosemary A. Stuart

Department of Biological Sciences, Marquette University
Milwaukee, WI

Abstract

Mitochondrial ribosomal protein 20 (Mrp20) is a component of the yeast mitochondrial large (54S) ribosomal subunit and is homologous to the bacterial L23 protein, located at the ribosomal tunnel exit site. The carboxy-terminal mitochondrial-specific domain of Mrp20 was found to have a crucial role in the assembly of the ribosomes. A new, membrane-bound, ribosomal-assembly subcomplex composed of known tunnel-exit-site proteins, an uncharacterized ribosomal protein, MrpL25, and the mitochondrial peroxiredoxin (Prx), Prx1, accumulates in an *mrp20ΔC* yeast mutant. Finally, data supporting the idea that the inner mitochondrial membrane acts as a platform for the ribosome assembly process are discussed.

Keywords

mitochondria, mitospecific domain, Mrp20, ribosome assembly, yeast

Introduction

Mitochondrial ribosomes have several similarities with their bacterial ancestors, in particular with respect to their protein composition and antibiotic sensitivities (Ban et al, 2000; Sharma et al, 2003; Smits et al, 2007). The mitochondrial ribosomes, however, synthesize only a small subset of proteins (eight in *Saccharomyces cerevisiae*). These are mainly integral membrane proteins, including essential proteins of the mitochondrial oxidative phosphorylation (OXPHOS) system (Borst & Grivell, 1978). Understanding of the assembly and function of mitochondrial ribosomes is thus important, because defects in mitochondrial-translation abilities underlie many human diseases that result in impaired OXPHOS capacities (O'Brien, 2002; Chrzanowska-Lightowlers et al, 2011).

Data indicate that all protein synthesis within the mitochondria is performed by membrane-anchored ribosomes, to ensure a close coupling between the protein-synthesis and membrane-insertion events (Spithill et al, 1978; Liu & Spremulli, 2000; Stuart, 2002; Fiori et al, 2003; Gruschke et al, 2010). By contrast, the bacterial ribosomes synthesize many diverse proteins—both soluble and integral membrane—and consequently both cytosolic and membrane-bound populations of ribosomes exist, and presumably cycle, within bacteria. How, and at what stage during the formation of translationally active ribosomes, mitochondrial ribosomal proteins become tethered to the inner membrane is unclear.

The molecular details of the mitochondrial ribosome-assembly pathway and the assembly factors involved are mostly uncharacterized. One report indicates that a late-stage assembly intermediate of the large (54S) ribosomal subunit, termed the pre54S particle, completes its assembly at the inner membrane, where it incorporates the mitochondrial ribosomal protein (Mrp)L32, proteolytically matured by the Yta10/Yta12 membrane protease (Nolden et al, 2005). Although it is thought to be a matrix-soluble

assembly intermediate, it has not yet been shown whether the assembly of the pre54S complex actually occurs in the matrix. It is also possible that the inner membrane, the ultimate site of ribosomal activity, functions as a platform to localize these assembly events.

In this study, we have focused on a large ribosomal subunit component termed the Mrp20 protein. Previous work using chemical crosslinking approaches has identified a network of proteins—Mrp20, MrpL4, MrpL40, MrpL27, MrpL22, MrpL13 and MrpL3—that are located near to the exit site of the polypeptide tunnel of the 54S particle in yeast (Jia et al, 2009; Gruschke et al, 2010). This network includes contact points for the association of the ribosomes with components of the inner membrane, Oxa1 and Mba1, that are involved with the membrane insertion of nascent chains (Jia et al, 2003, 2009; Ott et al, 2006; Gruschke et al, 2010). Mrp20 is homologous to the bacterial ribosomal protein L23 and it contains an extended carboxy-terminal region unique to its mitochondrial relatives, termed mitochondrial-specific or 'mitospecific' domain. Indeed, several mitochondrial ribosomal proteins differ from their bacterial ancestors by containing such mitospecific extensions, and the function of these diverse additional domains remains uncharacterized (Sharma et al, 2003; Smits et al, 2007).

Here, we demonstrate that the truncation of the mitospecific domain of Mrp20 has severe consequences for the assembly of translationally active ribosomes, and hence for the capacity of the cell to support OXPHOS activity and aerobic growth. Mitochondria harbouring the mutant Mrp20 protein accumulate a new membrane-bound ribosome-assembly subcomplex, enriched in proteins located near the exit site of the ribosomal polypeptide tunnel. On the basis of our findings, we propose that the inner mitochondrial membrane acts as a stage for ribosome-assembly events.

Results and Discussion

The Mrp20ΔC mutant has an OXPHOS defect

In addition to its L23 homology domain (residues 84–176), Mrp20 contains an extended C-terminal mitospecific domain (residues

176–263; Fig 1A). To investigate the functional relevance of this mitospecific domain, a yeast mutant (*mrp20ΔC*) harbouring a C-terminally truncated derivative of Mrp20 was created. The Mrp20ΔC protein has the final 23 residues removed, a deletion that was selected because it compromises a predicted α-helical domain at the C-terminus of Mrp20 (Fig 1A). Haploid *mrp20ΔC* yeast cells had a severe growth defect on glycerol-containing media, a non-fermentable carbon source, demonstrating their impaired ability to support aerobic respiration (Fig 1B). *In organello* translation in the presence of [^{35}S]methionine indicated that the *mrp20ΔC* mitochondria had a reduced ability to synthesize the mitochondrially encoded proteins, which include essential components of the OXPHOS complexes (Fig 1C). Failure to efficiently synthesize these proteins hinders the assembly, and thus the levels, of the OXPHOS complexes. Consistently, a strong reduction in the steady-state levels of OXPHOS-complex subunits was also observed in the *mrp20ΔC* mitochondria (Fig 1D). The levels of subunit 1 of the cytochrome *c* oxidase (Cox1), the Rieske FeS protein (of the cytochrome bc_1 complex) and ATP synthase subunit e—all OXPHOS-complex subunits, known to be susceptible to proteolytic turnover when the assembly of their respective complexes is prevented—were found to be drastically reduced in the *mrp20ΔC* mitochondria, similarly to that observed in the wild-type $ρ^0$ mitochondria (Fig 1D). The $ρ^0$ yeast strains are deficient in mitochondrial ribosomes and protein synthesis because they lack mitochondrial DNA (mtDNA) and thus the coding capacity for ribosomal RNA (rRNA).

Figure 1

The C-terminal region of Mrp20 protein is important for mitochondrial translation and oxidative-phosphorylation function. (**A**) The conserved L23 domain and the C-terminal mitospecific region that are truncated in the Mrp20ΔC derivative are indicated. (**B**) Serial 10-fold dilutions of WT, *mrp20ΔC* and GAL10-*Mrp20ΔC* cells were spotted on YPD, YPG or YPG supplemented with the minimal amount of galactose required to induce the GAL10 promoter (YPG+0.1% Gal) and grown at 30 °C. (**C**) *In organello* translation was monitored in WT, *mrp20ΔC* and GAL10-*Mrp20ΔC* mitochondria. Cox1, Cox2 and Cox3 of the cytochrome *c* oxidase; Atp6, Atp8 and Atp9 subunits of the F_1F_0-ATP synthase. (**D**) Steady-state levels of the OXPHOS subunits in the mitochondria (50 µg) isolated from the indicated strains. Tim17 was used as a loading control. Cyt*b*, cytochrome *b*; FeS, Rieske FeS protein; OXPHOS, oxidative phosphorylation; Su e, subunit e of the F_1F_0-ATP synthase; WT, wild type; YPD, YP plates containing glucose; YPG, YP plates containing glycerol.
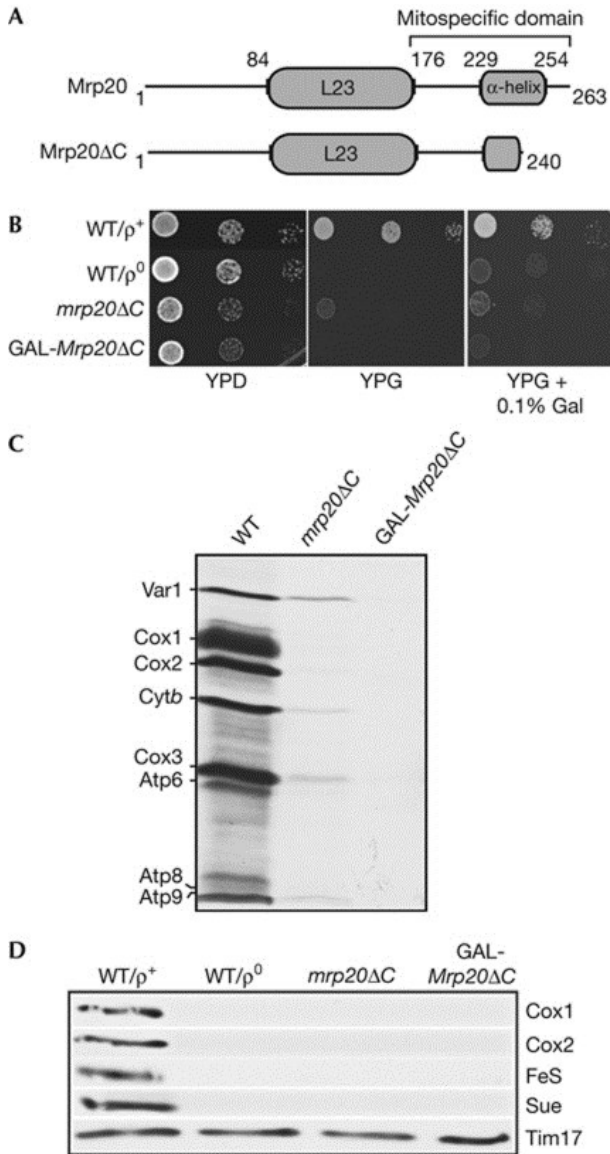
The mrp20ΔC mutant has a ribosome-assembly defect

The steady-state levels of the Mrp20ΔC protein in the *mrp20ΔC* mitochondria were reduced relative to the wild-type protein, indicating that the C-terminal truncation might have caused instability of the Mrp20 protein (Fig 2A). When the expression of the Mrp20ΔC protein in the *mrp20ΔC* mutant was placed under the control of the strong GAL10 promoter (GAL10-*Mrp20ΔC*), the steady-state level of the Mrp20ΔC protein was comparable with that of the full-length Mrp20 in

wild-type mitochondria ([Fig 2A](#)). Thus, elevated production of the mutant Mrp20ΔC protein compensated for its proposed proteolytic instability. Overexpression of the Mrp20ΔC protein in this manner did not overcome the defective translational activity of the *mrp20ΔC* mitochondria, and appeared to exacerbate it ([Fig 1C](#)). Consistently, the steady-state levels of the OXPHOS subunits remained severely compromised after overexpression of the Mrp20ΔC protein, and aerobic growth of the mutant remained severely affected ([Fig 1B,D](#)). Thus, taking the GAL10-*Mrp20ΔC* results together, we conclude that the translational defects observed in the *mrp20ΔC* mutant are not caused by the limiting levels of the Mrp20ΔC protein *per se*, but are instead directly caused by the consequences of the C-terminal truncation of the Mrp20 protein. It remains unclear why the GAL10-*Mrp20ΔC* mutant was more compromised in growth and translational activity than the *mrp20ΔC* mutant, despite the non-limiting levels of the Mrp20 protein.

Figure 2

The *mrp20ΔC* mutant has defective ribosome assembly. (**A**) Steady-state levels of ribosomal proteins in isolated mitochondria (50 μg) of the indicated strains. (**B**) Detergent-solubilized mitochondria from WT and GAL10-*mrp20ΔC* cells were subjected to sucrose-density sedimentation analysis. Immunodecoration of the resulting fractions (numbered from top to bottom) for indicated proteins was performed. (**C**) Haploid (mating type a) strains were crossed to a haploid WT/ρ^0 (mating type α) strain, followed by growth on YPD and YPG media (see [Fig 1B](#)). The Δ*oxa1* (YPG⁻/ρ^+) and the WT/ρ^0 (mating type a) strains were used as controls. (**D**) Detergent-solubilized GAL10-*mrp20ΔC* mitochondria were subjected to shallow sucrose-density sedimentation analysis using 5–25% sucrose gradients, and the resulting fractions were analysed further as described in **A**. The fractionation behaviour of control marker protein complexes harvested from a parallel sucrose gradient is indicated above with their mass (kDa). WT, wild type; YPD, YP plates containing glucose; YPG, YP plates containing glycerol.
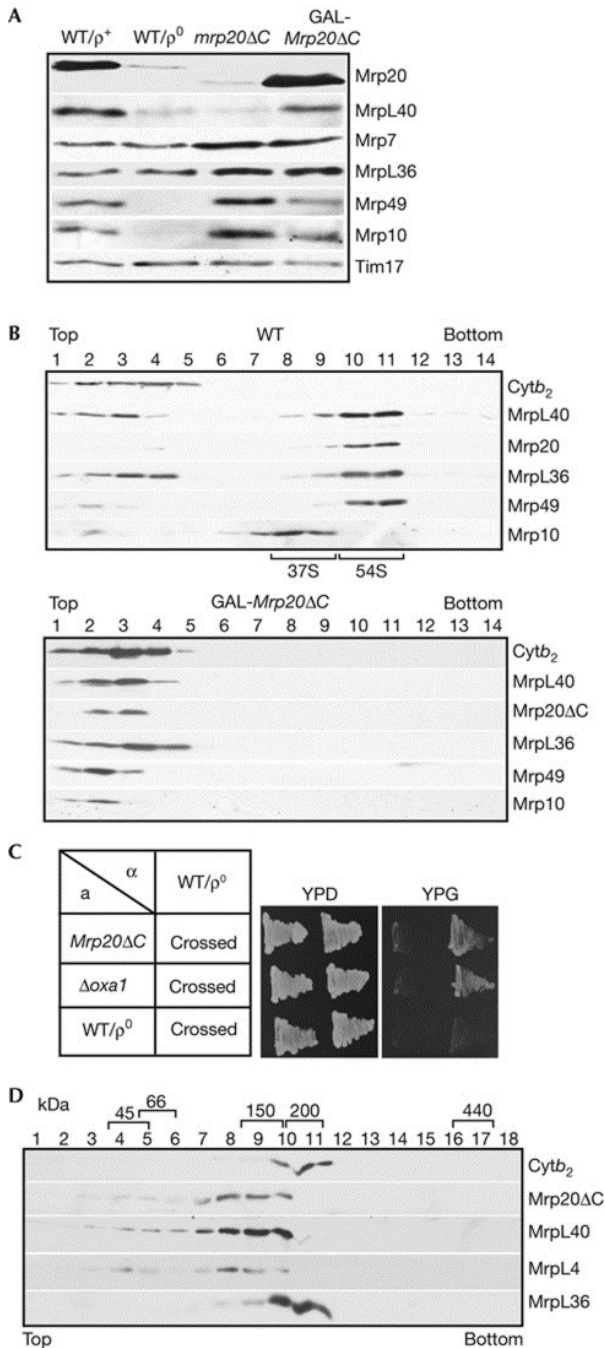
Due to the severely impaired mitochondrial translation, the assembly state of the ribosomes in the GAL10-*Mrp20ΔC* mitochondria was analysed ([Fig 2B](#)). In the wild-type, the assembly of the large ribosomal (54S) subunit was indicated by co-sedimentation of its components, MrpL40, Mrp20, MrpL36 and Mrp49, towards the bottom

of the gradient (Fig 2B). The small ribosomal (37S) subunit, as indicated by Mrp10, was recovered in fractions immediately before those containing the 54S proteins. In the GAL10-*Mrp20ΔC* mutant, the ribosomal proteins were all recovered towards the top of the gradient, indicating that they failed to assemble into a stable large ribosomal subunit (Fig 2B). Monitoring Mrp10 indicated a defect in the assembly of the small ribosomal subunit as well, suggesting that assembly of the large and small ribosomal subunits might not be independent processes. We conclude that truncation of the Mrp20 protein causes a defect in ribosome assembly, which in turn might account for the impaired translational abilities of these mitochondria.

Analysis of the levels of other ribosomal proteins in the *mrp20ΔC* and GAL10-*Mrp20ΔC* mitochondria indicated that, with the exception of MrpL40, they were similar, or elevated, in comparison with those of the wild-type mitochondria. This was in contrast to ρ^0 mitochondria, in which the levels of these ribosomal proteins are reduced because they are highly susceptible to proteolytic turnover in the absence of rRNA (Fig 2A). Yeast mutants defective in mitochondrial protein synthesis have been reported to lose their mtDNA with high frequency—that is, to change from ρ^+ to ρ^0/ρ^- status (Myers et al, 1985)—and thus the normal steady-state levels of the ribosomal proteins in the *mrp20ΔC* mutant were unexpected, given their lack of translational activity. When tested by genetic crossing, the *mrp20ΔC* mitochondria were, however, demonstrated to contain their mtDNA; they were ρ^+ (Fig 2C). Furthermore, both 21S and 15S rRNA were present in the *mrp20ΔC* mitochondria, although the level of 21S rRNA was slightly reduced when compared with the wild-type (supplementary Fig S1 online). Thus, the observed proteolytic stability of ribosomal proteins in the *mrp20ΔC* mitochondria might reflect that they have achieved at least a partial assembly state in the presence of the rRNA.

The levels of MrpL40 were decreased in the *mrp20ΔC* mitochondria, but elevated in the GAL10-*Mrp20ΔC* mitochondria (Fig 2A). MrpL40 is closely associated with the Mrp20 protein in the assembled ribosome (Jia et al, 2009; Gruschke et al, 2010), and these data suggest a dependence of MrpL40 on the Mrp20 protein—but not its extreme C-terminal region—for its stability.

Characterization of the Mrp20ΔC subcomplex

Taken together, our data indicate that truncation of the mitospecific domain of Mrp20 leads to a defect in ribosome assembly and hence translation. Due to the observed stability of the mtDNA, rRNA and ribosomal proteins, but the lack of stable 54S (or pre54S) particles, we propose that the defective stage of ribosome assembly in the *mrp20ΔC* mutant is downstream from that in ρ^0 mitochondria—in which ribosomal protein instability is observed—and upstream from the Δ*yta10* (or Δ*yta12*) mutant—in which the accumulation of stable pre54S particles is observed (Nolden et al, 2005). Thus, we conclude that the *mrp20ΔC* mutant represents a new type of ribosome-assembly mutant.

Sucrose-gradient centrifugation indicated that the detergent-solubilized Mrp20ΔC protein was present in a complex of approximately 150 kDa, which co-migrated with MrpL40 but separately from MrpL36 (Fig 2D). To identify further components of this Mrp20ΔC subcomplex, we expressed a C-terminally His-tagged derivative, Mrp20ΔC$_{His}$, in the *mrp20ΔC* strain (Fig 3A) and performed affinity purification using Ni-NTA (Ni-nitriloacetic acid) beads (Fig 3B). Several of other proteins were observed to specifically copurify with Mrp20ΔC$_{His}$ (Fig 3C). The indicated silver-stained bands were excised from the gel, and subjected to tryptic digestion and mass spectrometry analysis (supplementary Table S1 online). The analysis indicated these proteins to be MrpL40, MrpL4, MrpL25 and MrpL27, all large ribosomal proteins. In addition, one minor, but reproducible, band at approximately 28 kDa, was identified as peroxiredoxin 1 (Prx1), a mitochondrial peroxiredoxin protein. By using available antibodies, the specific recovery of MrpL40, MrpL4 and Prx1 with the Mrp20ΔC$_{His}$ protein was verified (Fig 3D). Recovery of members of this complex, such as MrpL40, with the purified Mrp20ΔC$_{His}$, reflected their physical association in the mitochondria before the lysis step, and was not due to their nonspecific association following detergent extraction (supplementary Fig S2 online). The association of MrpL25 and MrpL27 with the Mrp20ΔC subcomplex was independently tested by expressing His-tagged derivatives of these proteins in cells harbouring the non-tagged Mrp20ΔC protein (Fig 3E). The Mrp20ΔC, MrpL4 and MrpL40 proteins specifically copurified with both the MrpL25$_{His}$ and MrpL27$_{His}$

proteins from the *mrp20ΔC* mitochondria (Fig 3F). The ribosomal proteins MrpL36, Mrp7 and Mrp49 were not found in association with the Mrp20ΔC$_{His}$, MrpL25$_{His}$ or MrpL27$_{His}$ proteins, indicating that the Mrp20ΔC subcomplex was limited in its composition and does not contain all of the large ribosomal subunit proteins (Fig 3D,F). The Mrp20ΔC-subcomplex members Mrp20, MrpL4, MrpL40 and MrpL27 share a location within the 54S particle—the exit site of the ribosomal tunnel (Gruschke et al, 2010)—suggesting that this subcomplex might represent a true 54S assembly intermediate. MrpL25 is a mitochondria-specific ribosomal protein of unknown location in the ribosome (Smits et al, 2007), but its association with the Mrp20ΔC subcomplex suggests that it might be located near the tunnel exit site. MrpL36 and Mrp7 are homologues of bacterial L31 and L27 ribosomal proteins, respectively, large subunit components located at the small ribosomal subunit interface; far from the tunnel exit site (Smits et al, 2007). Their absence from the Mrp20ΔC subcomplex indicates that different regions of the large ribosomal subunit might independently assemble before the completion of the 54S particle. An intact mitospecific domain of Mrp20 is not required for the formation of the Mrp20ΔC subcomplex. The presence of an intact mitospecific domain of the Mrp20 protein, however, seems to be crucial for the interaction of this Mrp20 subcomplex with an assembly factor and/or with specific components of another ribosome assembly intermediate required to ensure the next step in the 54S assembly pathway.

Figure 3

Isolation of the *Mrp20ΔC* subcomplex. (**A**–**D**) Mitochondria isolated from WT or *mrp20ΔC* mutant expressing GAL10-driven Mrp20ΔC or Mrp20ΔC$_{His}$ proteins were analysed by SDS–PAGE, western blotting and immunedecoration with Mrp20- or His-specific antisera (**A**), or subjected to detergent solubilization and Ni-NTA purification, western blotting and immunedecoration (**B,D**) or silver staining (**C**). Total, 5% of the solubilized mitochondria; Bound, the Ni-NTA eluted material. (**E**–**G**) Mitochondria were isolated from WT, GAL10-*Mrp20ΔC,* GAL10-*Mrp20ΔC*$_{His}$ strains and GAL10-*Mrp20ΔC* strains expressing the His-tagged MrpL25 or MrpL27 (**E,F**) or Prx1$_{His}$ (**G**) proteins, as indicated. Following detergent solubilization, samples were subjected to Ni-NTA purification and further analysed as described in (**B**). MW, molecular weight; Prx, peroxiredoxin; SDS–PAGE, SDS–polyacrylamide gel electrophoresis; WT, wild type.
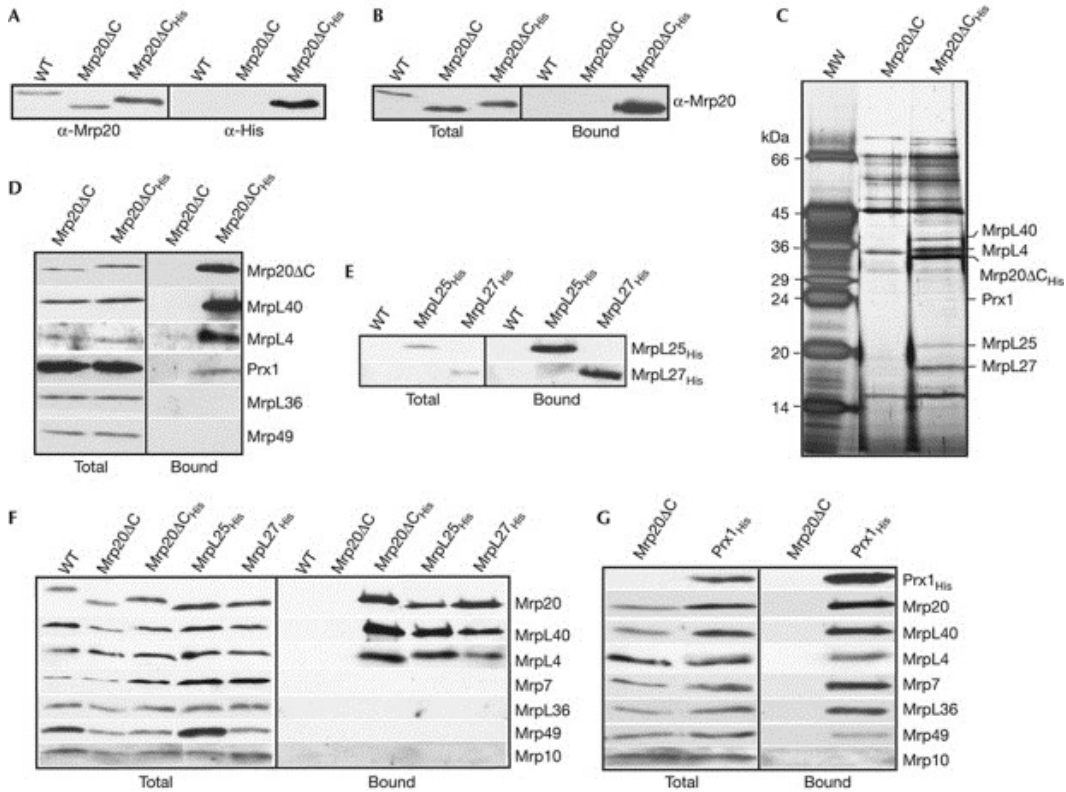
Finally, the proposed association of Prx1 with the Mrp20ΔC subcomplex was further analysed (Fig 3G). A C-terminally His-tagged Prx1 derivative, Prx1$_{His}$, copurified with the Mrp20ΔC, MrpL4 and MrpL40 proteins, further verifying the specificity of the Mrp20ΔC$_{His}$ results and the presence of Prx1 in the Mrp20ΔC subcomplex. Interestingly, other large ribosomal proteins—Mrp7, MrpL36 and Mrp49—were also specifically recovered with Prx1$_{His}$, suggesting that Prx1 can associate with more than one ribosomal subcomplex, and that it is not exclusively associated with the Mrp20ΔC subcomplex. Prx1 and its cytosolic homologue, Tsa1, have antioxidant-protective roles and Tsa1 can function to prevent the aggregation of ribosomal proteins under stress conditions (Trotter et al, 2008; Greetham & Grant, 2009). The association of Prx1 with diverse ribosomal subcomplexes indicates that it might function as an assembly chaperone or prevent oxidative damage during the assembly of ribosomal subcomplexes.

## *Mrp20ΔC subcomplex is tethered to the inner membrane*

The *mrp20ΔC* mutant accumulates a new ribosomal-assembly subcomplex composed of tunnel-exit-site proteins. To address whether this complex is membrane tethered in the absence of stable 54S assembly, *mrp20ΔC* mitochondria were subjected to a mild sonication treatment under low-salt conditions, followed by low-speed centrifugation to recover the mitochondrial membranes ([Fig 4A](#)). The ribosomal proteins, such as Mrp20ΔC, MrpL40 and MrpL36, all cofractionated with the inner-membrane marker, the ADP/ATP carrier protein and in a salt-sensitive manner. The soluble mitochondrial matrix protein Cpr3 was recovered exclusively in the supernatant fraction, indicating that the sonication conditions successfully disturbed the integrity of the mitochondrial membranes. The absence of ribosomal proteins in the supernatant indicated that the non-assembled ribosomal proteins in the *mrp20ΔC* mitochondria are not soluble proteins, but that they are membrane tethered ([Fig 4A](#)). Recovery of the ribosomal proteins in the pellet fraction was dependent on their association with the membrane, as when detergent was added to solubilize the membrane, the ribosomal proteins were released together with ADP/ATP carrier protein into the supernatant. A similar membrane-association behaviour of non-assembled ribosomal proteins was also observed in the ρ^0 mitochondrial sample ([Fig 4A](#)). In contrast to the full-length Mrp20 protein in ρ^0 mitochondria, a fraction of the Mrp20ΔC protein was recovered in the supernatant. Thus, the membrane association of Mrp20 might be partly compromised by truncation of its mitospecific domain ([Fig 4A](#)). When the membrane-bound fraction of Mrp20ΔC$_{His}$ was detergent extracted, it was found to be in association with components of the subcomplex, for example, MrpL40 and MrpL4 ([supplementary Fig S3](#) online). We therefore conclude that the Mrp20ΔC protein associated with the membrane is present in its subcomplex form.

Figure 4

Non-assembled ribosomal proteins are membrane associated. (**A**) Isolated GAL10-*mrp20ΔC* or WT/ρ^0 mitochondria were sonicated under different salt concentrations, and following the addition of Triton X-100 (1%), as indicated, were subjected to low-speed centrifugation. Membrane pellet (LP) and supernatant (S) fractions were

analysed by SDS–PAGE, western blotting and immunedecoration. Note that the exposure times for the WT/ρ⁰ blots were longer because of the reduced levels of ribosomal proteins in this mutant (see Fig 2B). (**B**) Mitochondria isolated from GAL10-*mrp20ΔC*, *Δyta10* and wild-type (WT/ρ⁺) strains were sonicated under low-salt conditions and subjected to membrane floatation assay. The resulting fractions were analysed further as described in (**A**). AAC, ADP/ATP carrier protein; SDS–PAGE, SDS–polyacrylamide gel electrophoresis; WT, wild type.
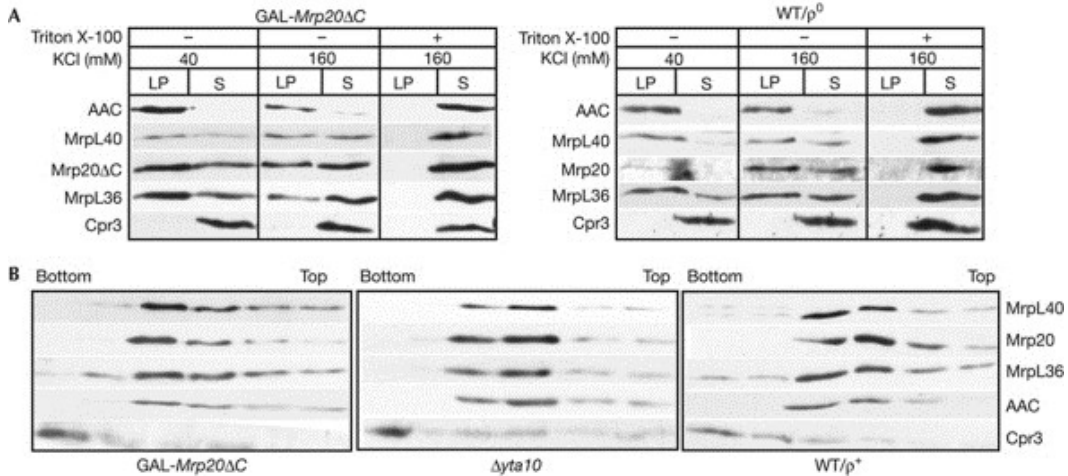
In an independent approach, membrane flotation was used to demonstrate the association of ribosomal proteins with membranes of mitochondria isolated from the *mrp20ΔC* and the late-stage ribosome assembly mutant, *Δyta10* strains (Fig 4B). Following sonication, mitochondrial samples were placed at the bottom of a sucrose gradient and subjected to ultra-centrifugation (Fig 4B). Soluble proteins—for example, Cpr3—are retained at the bottom of the gradient, whereas membrane-associated proteins—for example, ADP/ATP carrier protein—float up in the gradient. Flotation of ribosomal proteins with the inner membrane was observed in both the *mrp20ΔC* and *Δyta10* samples, in a manner that was similar to that reported previously for assembled ribosomes from wild-type mitochondria (Prestele et al, 2009; Fig 4B).

On the basis of the ρ⁰, *mrp20ΔC* and *Δyta10* data, we conclude that the association of these ribosomal proteins with the inner membrane is not dependent on the assembly of these proteins into a 54S (or pre54S) particle. We therefore propose that the process of mitochondrial ribosome assembly occurs on the surface of the inner

membrane, which is the site of ultimate translational activity. Staging the assembly process on the membrane circumvents the need to target an assembled matrix-localized large ribosomal subunit to the membrane when translation is required. It is possible that certain membrane proteins or lipids might form specialized ribosome-assembly sites in the membrane, to which ribosomal proteins become targeted after their import into mitochondria.

Methods

Subfractionation of mitochondria by sonication.

The mitoplasts (400 µg) were resuspended in 600 µl buffer A (20 mM HEPES-KOH, pH 7.4, 40 mM KCl (or 160 mM KCl, as indicated), 1 mM DTT and 1 mM PMSF), subjected to sonication on ice with a Branson sonifier 250 microtip (45% amplitude, five pulses of 6 s each interrupted by 90 s interval). For differential centrifugation analysis, the resulting sample was centrifuged for 10 min at 9,271g to give rise to a membrane pellet and supernatant fractions. For membrane flotation analysis, the sample was adjusted to 2.2 M sucrose (final volume 1 ml) and layered with (each 1 ml) 2, 1.5 and 1 M sucrose (in buffer A), and centrifuged for 16 h at 162,502 g at 2 °C (Beckman MLS-50 rotor).

Ni-NTA purification of His-tagged proteins.

Mitochondria (200 µg protein) were lysed in 200 µl of lysis buffer (20 mM HEPES-KOH, pH 7.4, 160 mM KCl, 1 mM PMSF and 1% Triton X-100) and Ni-NTA purification of His-tagged protein was performed, essentially as described previously (Jia et al, 2009).

Supplementary Material

Supplementary Information:

Supplementary Methods

Yeast strains.

Yeast strains used in this study were isogenic to W303-1A (Mat a, *leu2, trp1, ura3, his3, ade2*), ρ^0 W303-1A or W303-1B Mat a (or α, as indicated), *leu2, trp1, ura3, his3, ade2*), *mrpL40ΔC* and the *oxa1* null mutant, *Δoxa1::HIS3* (Jia *et al*, 2003; 2009). Homologous recombination was used to delete the codons 240-263 of MRP20 to generate the *mrp20ΔC* strain. Overexpression of the Mrp20ΔC, and His-tagged Mrp20ΔC, MrpL25 and MrpL27 proteins in *mrp20ΔC* (or *mrpL40ΔC* strain, as indicated) was achieved by cloning their respective genes into the Yip351 (Mrp20ΔC and Mrp20ΔC$_{His}$) or the Yip352 (other His-tagged proteins) vector system containing the galactose-inducible GAL10 promoter.

Sizing of Mrp20ΔC subcomplex by sucrose gradient centrifugation.

Isolated mitochondria (300µg) were solubilized with 300µl lysis buffer (1% Triton X-100, 20 mM HEPES-KOH pH-7.4, 160 mM KCl, 5 mM MgCl$_2$, 1 mM DTT, 1 mM PMSF) for 30 min on ice. The lysate was subjected to clarifying spin at 9271x g for 10 min at 4˚C. The supernatant was then layered onto an 11-ml continuous linear sucrose gradient (5-25%) and ultracentrifuged at 42,000 rpm for 12 hrs at 4˚C in Beckman SW41 Ti rotor. A second sucrose gradient was run in parallel, which contained a mixture of molecular weight marker proteins (ovalbumin, 45 kDa; bovine serum albumin, 66 kDa; alcohol dehydrogenase, 150 kDa; β-amylase, 200 kDa and apoferritin, 440 kDa). Fractions (550µl) were collected, TCA precipitated, and subjected to SDS-PAGE and Western blot analysis. The fractionation of the molecular mass markers was analyzed by Ponceau S staining.

Post-lysis control Ni-NTA purification experiment.

Mrp20ΔC$_{His}$ protein was expressed in a *mrpL40ΔC* mutant, a mutant where the levels of the truncated MrpL40 protein and endogenous Mrp20 have been previously shown to be extremely reduced (Jia *et al*, 2009). Mitochondria were isolated from this mutant (MrpL40ΔC+Mrp20ΔC$_{His}$; mitochondria #3 in Fig S3), as they represented as a source of the Mrp20ΔC$_{His}$ protein, which was not associated with full-length MrpL40 protein, and were used in the following post-lysis control experiment. Isolated mitochondria from the Mrp20ΔC (i.e. MrpL40-containing, but Mrp20ΔC$_{His}$ deficient mitochondria; #1 in Fig S3) and MrpL40ΔC+Mrp20ΔC$_{His}$ strains (each 100 μg protein) were mixed together prior to the detergent lysis step. Ni-NTA purification of the His-tagged Mrp20ΔC protein was performed as described earlier.

Ni-NTA purification of membrane bound Mrp20ΔC$_{His}$ protein.

Isolated mitochondria were sonicated in the presence of 40 mM KCl, and subjected to differential centrifugation (9,271 *x g*, 10 min, 4˚C) to give rise to a low speed pellet (LP) membrane and supernatant fraction, as described earlier. To analyze if the Mrp20ΔC$_{His}$ protein recovered in the LP membrane fraction existed in the subcomplex with other ribosomal proteins, the LP membrane fraction was pellet was subsequently solubilized with high salt lysis buffer (160 mM KCl, 20 mM HEPES-KOH, pH 7.4, 1% Triton X-100) and following a clarifying spin, Ni-NTA purification of the solubilized Mrp20ΔC$_{His}$ protein was performed, as previously described.

Mitochondrial rRNA isolation.

Mitochondrial RNA was extracted from isolated mitochondria using hot-acidic phenol extraction method, essentially as previously described (Zambrano *et al*, 2007). The RNA extracts were separated on a 1% agarose gel, stained with ethidium bromide, visualized under UV light and photographed. Purified acterial ribosomal rRNA (23S and 16S) was analyzed in parallel.

MALDI-TOF analysis and identification of Mrp20ΔC$_{His}$ co-purifying proteins.

The Ni-NTA purified Mrp20ΔC$_{His}$ protein complex was analyzed by SDS-PAGE followed by silver staining. The bands indicated in Fig. 3C were excised from the stained gel, subjected to tryptic digestion and are analyzed by mass spectrometry (Applied Biosystems Voyager-DE PRO MALDI-TOF mass spectrometer). This analysis was performed at the Protein and Nucleic Acid Facility at the Medical College of Wisconsin, Milwaukee. Protein identification was accomplished using searches against the Swiss-Prot protein sequence database. The resulting identifications are presented in Table S1.

Antisera used in this study.

Antisera against Cox2, Su e, MrpL40 were generated, as previously described (Jia *et al*, 2009). The following antisera were generously obtained from the following sources: MrpL36 and MrpL4 (Drs. J.M. Herrmann & M. Ott, Univ. Kaiserlautern), Mrp49 (Dr. M. Boguta, Polish Academy of Sciences, Warsaw), Mrp10 (Dr. A. Tzagoloff, Columbia Univ., New York), Prx1, (Dr. C. Grant, Manchester Univ.), Mrp20 and Mrp7 (Dr. T. Mason, Univ. Massachusetts, Amherst) and Tim17 (Dr. W. Neupert, Univ. Munich).

Miscellaneous.

Mitochondria were isolated from cultures grown at 30°C in YP-0.5 % lactate, 2% galactose media. Isolation of mitochondria and *in organello* labeling with [^{35}S]methionine, was performed essentially as described earlier (Jia *et al*, 2003; 2009). Standard procedures were used for SDS-PAGE and Western blotting. Sucrose gradient analysis of Triton X-100 solubilized mitochondrial ribosomes was performed as previously published (Jia *et al*, 2009). The data presented here in this paper represent typical results obtained in the various repeat experiments. Typically, each type of experiment presented here was performed at least 3 times, with similar results each time being obtained. Representative results are therefore shown. In many experiments, e.g. the Ni-NTA pull down experiments, the Western

blots following the SDSPAGE analysis were often cut into multiple strips, to enable the decoration with many independent antisera against proteins of different molecular masses. The figures therefore are a composite of the scans of the individual signals from these antibodies, as indicated in the figures.

Supplementary Reference

Zambrano A, Fontanesi F, Solans A, de Oliveira RL, Fox TD, Tzagoloff A, Barrientos A (2007) Aberrant translation of cytochrome *c* oxidase subunit 1 mRNA species in the absence of Mss51p in the yeast *Saccharomyces cerevisiae*. *Mol Biol Cell* **18:** 523-535

Supplementary figure legends

Figure S1
Presence of ribosomal RNA in the *mrp20ΔC* mutant. Mitochondrial rRNA (21S and 15S) was purified from isolated from wild type (WT) and *mrp20ΔC* mitochondria (20 μg mitochondrial protein) and analyzed by agarose electrophoresis, followed by staining with ethidium bromide and UV light visualization. Purified *E. coli* ribosomal rRNA (1 μg) (23S and 16S) was also analyzed in parallel.

Figure S2
The Mrp20ΔC$_{His}$ tagged protein does not associate with MrpL40 in a post-lysis manner. Mitochondria were isolated from the *mrpL40ΔC* mutant harboring the Mrp20ΔC$_{His}$ protein (MrpL40ΔC+Mrp20ΔC$_{His}$ #3) and were mixed prior to lysis with Gal-Mrp20ΔC mitochondria(#1), indicated by 1/3. Control Gal-Mrp20ΔC and Gal-Mrp20ΔC$_{His}$ (#2) mitochondria were also individually lysed in parallel. Following a clarifying spin, Ni-NTA purification was performed and samples analyzed by SDS-PAGE and Western blotting with Mrp20 and MrpL40 antibodies. Total, 5% of the solubilized mitochondria; Bound, the Ni-NTA eluted material. Note in sample #3, the levels of endogenous Mrp20 and MrpL40ΔC are below detection levels in the MrpL40ΔC+Mrp20ΔC$_{His}$ mitochondria and thus only His-tagged Mrp20ΔC can be observed in the "total". The MrpL40 protein detected in the "1/3" mixed sample, originates from the Gal-Mrp20ΔC mitochondria and does not bind to the Mrp20ΔC$_{His}$ protein from mitochondria #3 in a post-lysis manner.

Figure S3
Membrane associated Mrp20ΔC exists in subcomplex with the other ribosomal proteins. (A) Isolated mitochondria from GAL-*mrp20ΔC* and GAL-*mrp20ΔC*$_{His}$ strains were sonicated and subjected to low speed differential centrifugation. A fraction of the samples were removed to confirm efficient separation of the membranes (recovered in

the low speed pellet (LP) membrane fraction) from the soluble proteins (recovered in the supernatant fraction), was confirmed following SDS-PAGE analysis, Western blotting and immunedecoration. The ADP/ATP carrier protein (AAC) and Cpr3, served as markers for membrane and matrix-soluble proteins, respectively. (B) The remainder of the resulting membrane pellet (LP) was subsequently solubilized in high salt and detergent containing buffer and then subjected to the Ni-NTA purification. Samples were analyzed by Western blotting with ribosomal proteins. Total, 5% of the LP solubilized material; Bound, the Ni-NTA purified material.

Table S1 Mrp20ΔC$_{His}$ interacting proteins identified following SDS-PAGE, gel excision and mass spectrometry analysis

Protein assigned	Gene Name	Mr (kDa)[a]	Calculated pI[a]	Sequence Coverage (%)	Score[a]	Peptides Matched
Mitochondrial ribosomal protein MrpL4	YLR439w	37	7.69	47	2650	20
Mitochondrial ribosomal protein MrpL40	YPL173w	33.7	10.2	59	1000	14
Mitochondrial ribosomal protein Mrp20	YDR405w	30.5	10.2	47	2110	17
Peroxiredoxin, Prx1	YBL064c	29.5	9.47	40	203	9
Mitochondrial ribosomal protein MrpL25	YGR076c	18.6	9.85	41	158	9
Mitochondrial ribosomal protein MrpL27	YBR282w	16.5	10.96	52	530	10

[a] Calculated Mr (or pI) of precursor form
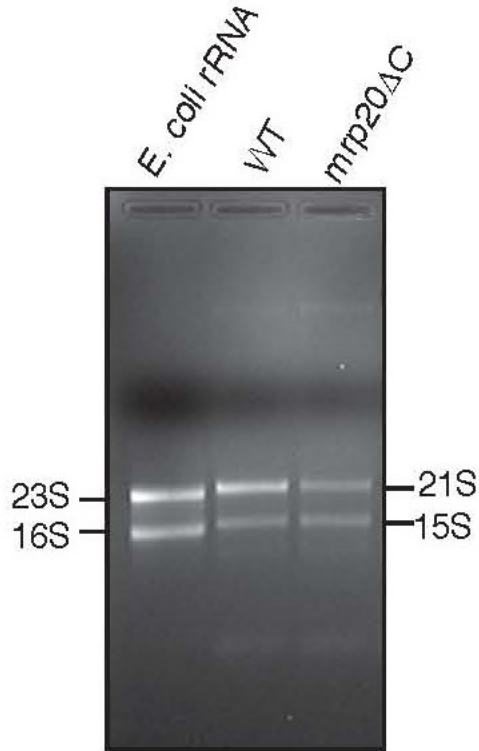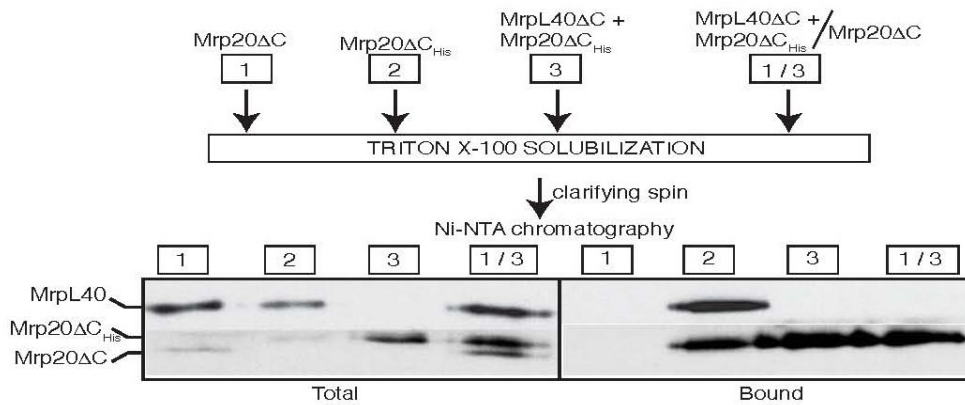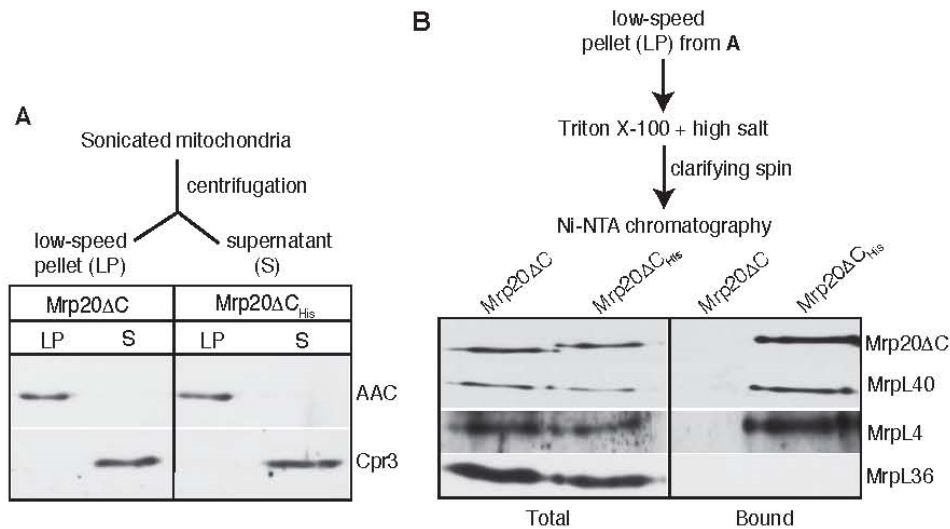[b] The Mowse scoring algorithm

Figure S1

Figure S2

Figure S3

Review Process File:

Truncation of the Mrp20 protein reveals novel ribosome assembly subcomplex in mitochondria

Jasvinder Kaur and Rosemary A. Stuart

Corresponding author: Rosemary A. Stuart, Marquette University

No Peer Review Process File is available with this article, as the authors have chosen not to make the review process public in this case.

Acknowledgments

Footnotes

The authors declare that they have no conflict of interest.

References

Ban N, Nissen P, Hansen J, Moore PB, Steitz TA (2000) The complete atomic structure of the large ribosomal subunit at 2.4 A resolution. Science 289: 905–920

Borst P, Grivell LA (1978) The mitochondrial genome of yeast. Cell 15: 705–723

Chrzanowska-Lightowlers ZMA, Horvath R, Lightowlers RN (2011) 175th ENMC International Workshop: mitochondrial protein synthesis in health and disease, 25–27th June 2010, Naarden, The Netherlands. Neuromusc Dis 21: 142–147

Fiori A, Mason TL, Fox TD (2003) Evidence that the synthesis of the *Saccharomyces cerevisiae* mitochondrially encoded ribosomal protein Var1p may be membrane localized. Eukaryot Cell 2: 651–653

Greetham D, Grant CM (2009) Antioxidant activity of the yeast mitochondrial one-Cys peroxiredoxin is dependent on thioredoxin reductase and glutathione *in vivo*. Mol Cell Biol 11: 3229–3240

Gruschke S, Grone K, Heublein M, Holz S, Israel L, Imhof A, Herrmann JM, Ott M (2010) Proteins at the polypeptide tunnel exit of the yeast mitochondrial ribosome. J Biol Chem 285: 19022–19028

Jia L, Dienhart M, Schramp M, McCauley M, Hell K, Stuart RA (2003) Yeast Oxa1 interacts with mitochondrial ribosomes: the importance of the C-terminal region of Oxa1. EMBO J 22: 6438–6447

Jia L, Kaur J, Stuart RA (2009) Mapping of the *Saccharomyces cerevisiae* Oxa1-mitochondrial ribosome interface and identification of MrpL40, a ribosomal protein in close proximity to Oxa1 and critical for oxidative phosphorylation complex assembly. Eukaryot Cell 8: 1792–1802

Liu M, Spremulli L (2000) Interaction of mammalian mitochondrial ribosomes with the inner membrane. J Biol Chem 275: 29400–29406

Myers AM, Pape LK, Tzagoloff A (1985) Mitochondrial protein synthesis is required for maintenance of intact mitochondrial genomes in *Saccharomyces cerevisiae*. EMBO J 4: 2087–2092

Nolden M, Ehses S, Koppen M, Bernacchia A, Rugarli EI, Langer T (2005) The m-AAA protease defective in hereditary spastic paraplegia controls ribosome assembly in mitochondria. Cell 123: 277–289

O'Brien TW (2002) Evolution of a protein-rich mitochondrial ribosome: implications for human genetic disease. Gene 286: 73–79

Ott M, Prestele M, Bauerschmitt H, Funes S, Bonnefoy N, Herrmann JM (2006) Mba1, a membrane-associated ribosome receptor in mitochondria. EMBO J 25: 1603–1610

Prestele M, Vogel F, Reichert AS, Herrmann JM, Ott M (2009) Mrpl36 is important for generation of assembly competent proteins during mitochondrial translation. Mol Biol Cell 20: 2615–2625

Sharma MR, Koc EC, Datta PP, Booth TM, Spremulli LL, Agrawal RK (2003) Structure of the mammalian mitochondrial ribosome reveals an expanded functional role for its component proteins. Cell 115: 97–108

Smits P, Smeitink JA, van den Heuvel LP, Huynen MA, Ettema TJ (2007) Reconstructing the evolution of the mitochondrial ribosomal proteome. Nucleic Acids Res 35: 4686–4703 [

Spithill TW, Trembath MK, Lukins HB, Linnane AW (1978) Mutations of the mitochondrial DNA of *Saccharomyces cerevisiae* which affect the interaction between mitochondrial ribosomes and the inner mitochondrial membrane. Mol Gen Genet 164: 155–162

Stuart RA (2002) Insertion of proteins into the inner membrane of mitochondria: the role of the Oxa1 complex. Biochim Biophys Acta 1592: 79–87

Trotter EW, Rand JD, Vickerstaff J, Grant CM (2008) The yeast Tsa1 peroxiredoxin is a ribosome-associated antioxidant. Biochem J 412: 73–80